Vision, Modeling, and Visualization (2013)
Michael Bronstein, Jean Favre, and Kai Hormann (Eds.)

A Thin Shell Approach to the Registration of Implicit Surfaces

J. A. Iglesias[1], B. Berkels[2,3], M. Rumpf[2] and O. Scherzer[1,4]

[1]Computational Science Center, University of Vienna, Austria
[2]Institute for Numerical Simulation, University of Bonn, Germany
[3]Institute of Mathematics and Image Computing, University of Lübeck, Germany
[4]Radon Institute of Computational and Applied Mathematics, Austrian Academy of Sciences, Linz, Austria

Abstract

Frequently, one aims at the co-registration of geometries described implicitly by images as level sets. This paper proposes a novel shape sensitive approach for the matching of such implicit surfaces. Motivated by physical models of elastic shells a variational approach is proposed, which distinguishes two different types of energy contributions: a membrane energy measuring the rate of tangential distortion when deforming the reference surface into the template surface, and a bending energy reflecting the required amount of bending. The variational model is formulated via a narrow band approach. The built in tangential distortion energy leads to a suitable equidistribution of deformed length and area elements, under the optimal matching deformation, whereas the minimization of the bending energy fosters a proper matching of shape features such as crests, valleys or bumps. In the implementation, a spatial discretization via finite elements, a nonlinear conjugate gradient scheme with a Sobolev metric, and a cascadic multilevel optimization strategy are used. The features of the proposed method are discussed via applications both for synthetic and realistic examples.

Categories and Subject Descriptors (according to ACM CCS):
I.3.5 [Computer Graphics]: Computational Geometry and Object Modeling—Boundary representations
I.4.3 [Image Processing and Computer Vision]: Enhancement—Registration

1. Introduction and motivation

We address the problem of matching closed surfaces or curves, which are given as the zero level sets of functions defined in a volume or a planar domain. In vision many geometric objects are actually extracted from images as level sets. Furthermore, formulating geometric problems in terms of level sets often simplifies their numerical implementation, since regular grids can be used. As a consequence, we look for deformations of the whole computational domain which closely match a template surface to a reference surface, are invertible both on the surfaces and globally, and match geometric features (e.g. curvatures) of the surfaces while having low tangential distortion. For the mathematical modeling, we think of the reference surface as a layer of an elastic material (for example, rubber) embedded in a block of another much softer isotropic elastic material (foam, say), subject to a matching force that forces it onto the template surface.

With this in mind we derive a variational formulation motivated from the standard mathematical theories of nonlinear elasticity. However, our model is different from them in some aspects, to better exploit the specific advantages of our matching scenario, not present in physical situations. We will point out both the similarities and differences as we introduce and motivate the different parts of our energy.

2. Related work

In recent years, theories of nonlinear elasticity have found use in many problems of computer vision and graphics. Some applications are deformation of meshes [CPSS10], shape averages and geodesics between shapes [RW09, WBRS11], and registration of medical images [BMR13]. In the last work, the efficient discretization and numerical solution of hyperelastic regularization energies is studied. The chosen approach is a cascadic minimization scheme involving a Gauss-Newton method on each level.

Linear elasticity is also used for image registration

DOI: 10.2312/PE.VMV.VMV13.089-096

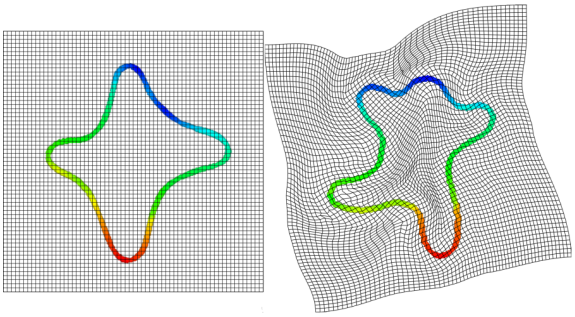

Figure 1: *Result obtained with our method, when used for curves in a 2D domain. We look for a global and invertible deformation, which closely matches two input shapes, in a way that balances being as isometric as possible on the shapes, and matching their curvatures. On the left the reference shape is shown on the undeformed grid, whereas on the right the deformed reference shape matching the given template shape is rendered together with the deformed mesh. Undeformed and deformed points are colored identically.*

[Mod04] and shape modeling [FJSY09], but the advantage of nonlinear models is that they allow for intuitive deformations when the displacements are large.

In this paper, the focus is on nonlinear elastic matching of thin shells. A finite element method for the discretization of bending energies of thin shell type biological interfaces has been studied in [BNP10]. Their approach uses quadratic isoparametric finite elements to handle the interface on which an elastic energy of Helfrich type is approximated. In [SSJD09], face matching based on a matching of corresponding level set curves on the facial surfaces is investigated. To match pairs of curves an optimal deformation between them is computed using an elastic shape analysis of curves. Compared to our approach, this model does not take into account dissipation along deformation paths caused by a bending of the curves. The paper [BPW12] discusses a new concept for the treatment of higher order variational problems on surfaces described as jump sets of functions of bounded variation type. This approach in particular enables the analytical rigorous treatment of elastic energies on such surfaces. The matching of surfaces with elastic energies has recently been studied in [WSSC11]. Their energy splits into a membrane energy depending on the Cauchy-Green strain tensor and a bending energy, comparing only the mean curvatures on the surfaces. The matching problem is phrased in terms of a binary linear program in the product space of sets of surface patches. A relaxation approach is used to render it computationally feasible. An approach related to ours is presented in [LDRS05], where nonlinear elastic energies are proposed for matching of open, parametrized surface patches. Here, we propose a method for closed surfaces that does not require a parametrization.

A method for matching and blending represented by level sets has been presented in [MR12]. A level set evolution generates an interpolating family of curves, where the associated propagation speed of the level sets depends on differences of level set curvatures. In this class of approaches, geometric evolution problems are formulated, whereas here we focus on variational models for matching deformations. Registration of implicit surfaces was considered in [LL08], but only through volumetric terms, in contrast to our tangential distortion and bending terms.

Let us mention that our approach is inspired by the works [DZ94, DZ95] in which partial differential equations for shell models are derived in terms of distance functions. Shape warping based on the framework of [DZ94] from a less physical perspective has been discussed in [CFK04].

3. A thin shell matching model

Our model for the shape sensitive matching of surfaces is based on physical models for the elastic deformation of a thin shell [Cia00]. Thereby, a shell $\mathcal{M}$ is considered as the $d-1$ dimensional mid-surface of a layer of material of thickness $\delta << 1$ in $\mathbb{R}^d$.

To match two shell surfaces $\mathcal{M}_1$ and $\mathcal{M}_2$ via a deformation ϕ, we take into account the elastic energy of a deformation $\phi : \mathcal{M}_1 \to \mathbb{R}^3$ under the constraint $\phi(\mathcal{M}_1) = \mathcal{M}_2$. The energy can be decomposed into a membrane energy (penalizing stretching and compression strain) and a bending energy (penalizing strain caused by bending). Under this constraint the energy actually depends only on the Jacobian of the deformation ϕ and not on second derivatives of ϕ, since curvatures for the bending term can be evaluated on $\mathcal{M}_2$.

Membrane energy. The rate of tangential distortion at each point is described by the tangential Cauchy-Green strain tensor (cf. Figure 2)

$$A_{\mathrm{tg}}[\phi] = D_{\mathrm{tg}}\phi^T D_{\mathrm{tg}}\phi.$$

Here, the tangential Jacobian of the deformation is defined by $D_{\mathrm{tg}}\phi = D\phi^{ext}P$ for an extension ϕ^{ext} of ϕ onto a neighborhood of $\mathcal{M}_1$, $P = \mathrm{Id} - N_1 \otimes N_1$ being the projection onto the tangent space of $\mathcal{M}_1$ with normal N_1. Then, the associated membrane energy is given by

$$\mathcal{E}_{\mathrm{mem}}[\phi] = \delta \int_{\mathcal{M}_1} W_{\mathrm{mem}}(A_{\mathrm{tg}}[\phi])\,\mathrm{d}a\,, \tag{1}$$

where we choose as the requisite energy density

$$W_{\mathrm{mem}}(A) = \frac{\mu}{2}\,\mathrm{tr}A + \frac{\lambda - 2\mu}{8}\,\det A + \frac{2\mu+\lambda}{8}(\det A)^{-1}. \tag{2}$$

Here, λ and μ are the Lamé constants of a St. Venant–Kirchhoff material [Cia88] with $\mathrm{tr}A$ and $\det A$ denoting the trace and the determinant of A considered as an endomorphism on the tangent bundle of $\mathcal{M}_1$. Notice that $\det A$ describes area distortion, while $\mathrm{tr}A$ measures length distortion.

The polyconvex function W_{mem} is rigid body motion invariant, and it can be verified, using the invariance, that the identity is its only minimizer. Furthermore, the second order Taylor expansion at the identity reveals the classical quadratic energy of linearized, isotropic elasticity.

A simplification of the functional in (1) corresponds to the known Γ-limit of volume elasticity models for vanishing thickness parameter δ [LDR96]. This limit does not account for compression resistance [FJM06]. In our case, the energy density (2) does reflect compression resistance through the term involving $(\det A)^{-1}$, which also avoids self interpenetration, thus giving a more precise physical model.

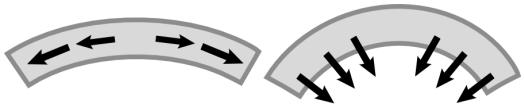

Figure 2: *A sketch of the two different modes of deformation of a thin shell: tangential distortion (left) and bending (right)*

Bending energy. The bending energy measures the local rate of bending described by the change of curvature under the deformation (cf. Figure 2). The shape operator of $\mathcal{M}_i$ is defined as the tangential Jacobian $D_{\text{tg}}N_i$ of the normal N_i. From the fact that $0 = \partial_k \|N_i\|^2 = 2\partial_k N_i \cdot N_i$, one deduces that $(D_{\text{tg}}N_i)(x)$ is an endomorphism of the tangent space $T_x\mathcal{M}_i$. Aiming at a comparison of $D_{\text{tg}}N_1$ at some point $x \in \mathcal{M}_1$ and $D_{\text{tg}}N_2$ at the deformed position $\phi(x)$, we have to use a corresponding pullback under the deformation ϕ and with it define the relative shape operator

$$S_{rel}[\phi](x) := D_{\text{tg}}\phi^T (D_{\text{tg}}N_2)(\phi(x)) D_{\text{tg}}\phi - (D_{\text{tg}}N_1)(x).$$

If ϕ is an isometric deformation of the shell $\mathcal{M}_1$, i.e. $A_{\text{tg}}[\phi](x) = \text{Id}_{T_x\mathcal{M}_1}$, then we recover the definition of the relative shape operator used in the rigorous analysis in Friesecke et al. [FJMM03]. In this case, the leading order term of the bending energy as the Γ-limit of 3D elasticity is *cubic* in the thickness δ and given by

$$\mathcal{E}_{\text{bend}}[\phi] = \delta^3 \int_{\mathcal{M}_1} W_{\text{bend}}(S_{rel}[\phi])\, \mathrm{d}a\,. \tag{3}$$

Although other choices are conceivable, we consider $W_{\text{bend}}(S) = \|S\|_F^2$, where $\|S(x)\|_F$ denotes the Frobenius norm of the corresponding linear operator $S(x) : T_x\mathcal{M} \to T_x\mathcal{M}$. Notice that different from bending energies considered in graphics elsewhere, $S_{rel}[\phi]$ takes into account the full change of the shape operators on $\mathcal{M}_1$ and $\mathcal{M}_2$, not only the change of their traces (i.e. mean curvatures), so that changes of bending *directions* get accounted for appropriately.

Deformation energy. Combining membrane (1) and bending (3) contributions, we obtain the total elastic shell energy

$$\mathcal{E}_{\text{sh}}[\phi] = \alpha_{\text{bend}}\mathcal{E}_{\text{bend}}[\phi] + \alpha_{\text{mem}}\mathcal{E}_{\text{mem}}[\phi]\,. \tag{4}$$

A fundamental insight arising from the analysis of shell models [Cia00] and the recent advances in a rigorous limit theory [LDR96, FJMM03] is that pure membrane terms and pure bending terms cannot coexist in the limit of zero thickness, since the scaling of these terms with respect to it is governed by a different power of the width of the shell δ. However, because of their distinct properties, in shape matching applications it is beneficial to use both, in particular considering the bending energy of non-isometric deformations. This formulation is the basis for our level set method for surface matching discussed in the next section.

4. Level set framework

Now we derive the actual variational approach for the matching of implicit surfaces. To this end, we suppose that the geometries $\mathcal{M}_1$ and $\mathcal{M}_2$ are implicitly described hypersurfaces on a computational domain $\Omega \subset \mathbb{R}^d$ (curves for $d = 2$ and surfaces for $d = 3$). Explicitly, we assume $\mathcal{M}_i$ to be described by its signed distance function $\mathbf{d}_i$, which constitute our input data (cf. Figure 3). For closed surfaces our convention is that $\mathbf{d}_i$ is positive outside $\mathcal{M}_i$. If the input is not a distance function but any other regular level set function, one can obtain a distance function via the application of the fast marching method [Set99]. For any c, we denote the c-offsets to these surfaces by $\mathcal{M}_i^c = \{x \in D \,|\, \mathbf{d}_i(x) = c\}$. In what follows, we consider a deformation $\phi : D \mapsto \mathbb{R}^3$, which approximately maps $\mathcal{M}_1$ onto $\mathcal{M}_2$. Since the $\mathbf{d}_i$ are distance functions, we have $|\nabla \mathbf{d}_i| = 1$, so that $\nabla \mathbf{d}_i(x)$ is the unit normal to $\mathcal{M}_i^{\mathbf{d}_i(x)}$ at a point x. Then, the tangent space to $\mathcal{M}_i^{\mathbf{d}_i(x)}$ at x, denoted by $T_x\mathcal{M}_i^{\mathbf{d}_i(x)}$, consists of all vectors orthogonal to $\nabla \mathbf{d}_i(x)$. Projection matrices onto these tangent spaces can be computed by $P_i(x) = \text{Id} - \nabla \mathbf{d}_i(x) \otimes \nabla \mathbf{d}_i(x)$, which induce, on the whole domain, the tangential derivative $D_{\text{tg}}\phi(x) = D\phi(x)P_1(x)$ of the deformation and the tangential Cauchy-Green strain tensor $A_{\text{tg}}[\phi] = D_{\text{tg}}\phi^T D_{\text{tg}}\phi$ to each level set. Analogously, we can also compute the shape operators of $\mathcal{M}_1^{\mathbf{d}_1(x)}$ at x and $\mathcal{M}_2^{\mathbf{d}_2(\phi(x))}$ at $\phi(x)$ through $\mathcal{S}_1(x) = D^2\mathbf{d}_i(x)$ and $\mathcal{S}_2(x) = D^2\mathbf{d}_2(\phi(x))$. We can then use these level set expressions in the energies (1) and (3), to

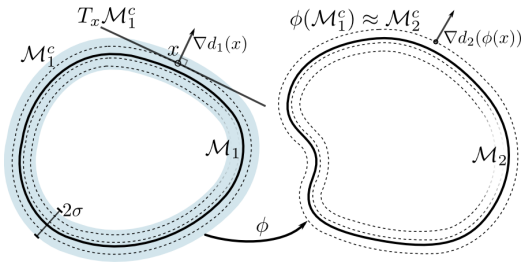

Figure 3: *A sketch of the level set framework with the narrow band around the surface $\mathcal{M}_1$ marked in light blue. The dashed lines on the left indicate different level sets of $\mathbf{d}_1$ (left) and there deformed images (right).*

rewrite the components of the shell energies on a single level set in terms of the deformation and the two signed distance functions $\mathbf{d}_1$ and $\mathbf{d}_2$. In what follows, we will combine this with a narrow band approach focusing on a small neighborhood of the actual surfaces of interest.

Narrow band formulation of shell energies. As is customary in level set methods [Set99], we introduce a narrow band around $\mathcal{M}_1$, whose deformation we want to capture (cf. Figure 3). This is done by a smooth and even cutoff function η_σ such that $\eta_\sigma(0) = 1$ and $\eta_\sigma(s) = 0$ if $|s| > \sigma$. The support of the composition $\eta_\sigma \circ \mathbf{d}_1$ then identifies the narrow band.

To formulate a level set variational method, we measure the distortion created by the deformation ϕ on each level set $\mathcal{M}_1^c$ through the shell energy (4), obtaining $\mathcal{E}_{\mathrm{sh}}^c[\phi] = \int_{\mathcal{M}_1^c} W_{\mathrm{sh}}[\phi]\,\mathrm{d}a$. Here, the energy density $W_{\mathrm{sh}}[\phi]$ expressed in terms of $\mathbf{d}_1$, $\mathbf{d}_2$ and ϕ is given by

$$W_{\mathrm{sh}}[\phi] = \alpha_{\mathrm{mem}}\delta W_{\mathrm{mem}}(A_{\mathrm{tg}}[\phi]) + \alpha_{\mathrm{bend}}\delta^3 W_{\mathrm{bend}}(S_{rel}[\phi]),$$

where $A_{\mathrm{tg}}[\phi] = D_{\mathrm{tg}}\phi^T D_{\mathrm{tg}}\phi$ is the tangential Cauchy-Green strain tensor, with $D_{\mathrm{tg}}\phi = D\phi(\mathrm{Id} - \nabla\mathbf{d}_i \otimes \nabla\mathbf{d}_i)$ denoting the tangential derivative of the deformation, and $S_{rel}[\phi] = D_{\mathrm{tg}}\phi^T\,(D^2\mathbf{d}_2 \circ \phi)\,D_{\mathrm{tg}}\phi - D^2\mathbf{d}_1$ is the relative shape operator expressed in terms of the distance functions and the deformation. Now, we weight this energy by $\eta_\sigma(c)$ and use the coarea formula [EG92] (using once again that $|\nabla\mathbf{d}_1| = 1$) to integrate the resulting weighted energy over all level sets of interest and obtain

$$\mathcal{E}_{\mathrm{sh}}[\phi] = \int_{-\infty}^{+\infty} \mathcal{E}_{\mathrm{sh}}^c[\phi]\,dc = \int_\Omega \eta_\sigma(\mathbf{d}_1) W_{\mathrm{sh}}[\phi]\,\mathrm{d}x. \quad (5)$$

In this manner we are able to define a global energy, defined as a volume integral over the computational domain, consistent with the surface energy defined on each of the offsets $\mathcal{M}_1^c$ which fill up the narrow band.

Handling the constraint. In our shell model, we have assumed that $\phi(\mathcal{M}_1^c) = \mathcal{M}_2^c$. This allows us to formulate the bending energy in terms of the shape operators of the given surfaces $\mathcal{M}_1^c$ and $\mathcal{M}_2^c$ for $|c| \le \sigma$. In practice, we use a quadratic penalty on the surface $\mathcal{M}_1^c$ measuring the difference between the deformed distance function $\mathbf{d}_2 \circ \phi$ and the desired distance value c, leading to the functional $\frac{1}{\varepsilon}\int_{\mathcal{M}_1^c} |\mathbf{d}_2 \circ \phi - c|^2\,da$ for some small $\varepsilon > 0$. Again using the coarea formula we obtain the global mismatch penalty

$$\mathcal{E}_{\mathrm{mismatch}}[\phi] = \frac{1}{\varepsilon}\int_\Omega \eta_\sigma(\mathbf{d}_1)|\mathbf{d}_2 \circ \phi - \mathbf{d}_1|^2\,\mathrm{d}x, \quad (6)$$

which amounts to the squared L^2 distance of the pullback of $\mathbf{d}_2$ under the deformation ϕ and $\mathbf{d}_1$, weighted at each level set by η_σ.

Volumetric hyperelastic regularization. So far the resulting energy does not impose any restriction on the deformation outside the narrow band of thickness 2σ around $\mathcal{M}_1$. Thus, to obtain a well-posed variational model on the whole computational domain, we have to take into account some regularization functional outside the narrow band. To this end, we add an additional volumetric elastic energy evaluated on the deformation ϕ. Following the usual paradigms of nonlinear elasticity, we choose

$$\mathcal{E}_{\mathrm{vol}}[\phi] = \xi\int_\Omega W_{\mathrm{vol}}(A[\phi])\,\mathrm{d}x \quad (7)$$

for $\xi > 0$ small, where $A[\phi] = D\phi^T D\phi$ is the usual Cauchy-Green strain tensor. The requisite energy density is given by

$$W_{\mathrm{vol}}(A) = \frac{\tilde\mu}{2}\,\mathrm{tr}A + \frac{\tilde\lambda - 2\tilde\mu}{8}\,\det A + \frac{2\tilde\mu + \tilde\lambda}{8}(\det A)^{-1} \quad (8)$$

for the Lamé constants $\tilde\lambda$ and $\tilde\mu$ of a St. Venant–Kirchhoff material. Notice that the difference with respect to the membrane energy (1) is the use of the three-dimensional strain tensor A, instead of A_{tg}. Physically, the resulting energy corresponds to a soft elastic material outside the narrow band in which the comparatively rigid surfaces inside the band are embedded. The addition of this term ensures that the obtained transformations are invertible on the whole domain, and this in turn implies that the deformed surfaces will not collapse and intersect themselves, a problem that can not be prevented with a tangential energy density alone.

We can alternatively consider the surfaces $\mathcal{M}_1$ and $\mathcal{M}_2$ as boundaries of volumetric objects, i.e. modelling elastic bodies those contours are themselves elastic shells, through

$$\mathcal{E}_{\mathrm{vol}}[\phi] = \int_\Omega \left(\zeta + (1-\zeta)\chi_{\{\mathbf{d}_1<0\}}\right) W_{\mathrm{vol}}[\phi]\,\mathrm{d}x. \quad (9)$$

The registration energy. Combining the above energy terms we obtain the total thin shell registration energy for implicit surfaces

$$\mathcal{E}_{\mathrm{total}}[\phi] = \mathcal{E}_{\mathrm{sh}}[\phi] + \mathcal{E}_{\mathrm{mismatch}}[\phi] + \mathcal{E}_{\mathrm{vol}}[\phi].$$

The numerical method for the minimization of this energy will be discussed in the following section.

5. Discretization and minimization

In the level set framework investigated here, we can use a straightforward space discretization to solve the problem numerically. Since the problem only includes first order derivatives of ϕ in the energy, we take into account multi-linear finite elements for the spatial discretization of the involved energy and run an optimization method on the coefficients of the solution in this finite element basis.

Computation of the curvatures. However, we also need to compute curvatures from the distance functions $\mathbf{d}_i$ given as data, i.e. we have to robustly compute a suitable approximation of $D^2\mathbf{d}_i$ to evaluate the shape operators. Furthermore, first derivatives of these functions have to computed when the gradient of the energy is needed in the descent method. Our approach, similar to the one used in [PR02],

is to compute these derivative matrices by projection onto quadratic polynomials spanned in a local neighborhood of each point. In explicit, for each node x_k we consider the set of nodes x_j in the r neighborhood $B_r(x_k)$ of x_k and compute the quadratic polynomial $x \mapsto p_k(x)$ which minimizes

$$\sum_{x_j \in B_r(x_k)} \left(p_k(x_j) - \mathbf{d}_i^j \right)^2 .$$

To solve this quadratic minimization problem, we have to solve a small linear system for every node x_k. The associated system matrix is independent of the node x_k on the regular grid lattice. Thus, we can precompute the LR decomposition of the matrix. Once the polynomial coefficients are computed, we replace the Hessian of $\mathbf{d}_i$ at every node x_k in our matching model by the Hessian of the polynomial p_k.

Cascadic multilevel descent. Because we are solving a highly nonlinear and non convex registration problem, we apply the standard paradigm of a coarse-to-fine cascadic minimization. Let us suppose that a dyadic scale of a regular mesh is given, where the grid is is divided by two on each level of the hierarchy. For the minimization at each level, we used a Fletcher-Reeves nonlinear conjugate gradient method (see [NW06], section 5.2), in which the gradients are computed with respect to a Sobolev metric by $\mathrm{grad}_{H^1} E[\phi] = (1 - \frac{\beta^2}{2}\Delta)^{-1} \mathrm{grad}_{L^2} E[\phi]$, where $\mathrm{grad}_{L^2} E[\phi]$ is the usual L^2 gradient appearing in the Euler-Lagrange equation. This amounts to smoothing the descent directions by an approximation of a Gaussian with filter width β. As indicated in Algorithm 1, the smoothing is reduced gradually to be able to capture details of the deformation.

Algorithm 1 Coarse-to-fine Sobolev descent

```
φ ← Id
for l ← l_min to l_max do
    h ← 1/(2^l + 1)
    β ← β_max
    while α > β_min do
        φ ← Sobolev-CG-descent (β, φ)
        β ← β/2
    end while
end for
return φ
```

Parameter choices. Despite the many parameters present in the energy, the underlying physical intuition of the model allows to make judicious choices without much effort. We indicate some example ranges, which were used in all the applications presented. The material properties $\alpha_{\mathrm{mem}}, \alpha_{\mathrm{bend}}$ of the shell in (4) were the 'reference parameters', and were taken to be ≈ 1. One can choose then $\lambda \approx 2, \mu \approx 0.25$. In comparison ε^{-1} in (6) should be large, and was taken to be $\approx 10^3$. The outside parameters should correspond to a comparably soft material, so picking $\tilde{\lambda} = \lambda, \tilde{\mu} = \mu$ and $\xi \approx 10^{-3}$ for (7) was sufficient. The bending energy (3) turned out to have enough influence to induce correct matchings with a shell width parameter $\delta = 0.5$. Additionally, we varied the parameters ε and δ when changing from a coarser to the next finer level by a factor 0.5, the above values being used on the coarsest grid level. This proved to be a very suitable strategy to ensure that $\mathcal{M}_1$ and $\mathcal{M}_2$ are appropriately matched at all scales, and that geometric details are actually resolved under the deformation on the finest grid level.

6. Results

We demonstrate the properties of our method with some numerical results. First, we depict some interesting qualitative properties of our models. Afterwards, we show some real applications for the matching of two dimensional surfaces.

Redistribution of tangential distortion. Here we aim to experimentally confirm that the membrane term (1) redistributes the tangential strain which necessarily occurs when shapes of different length or area are matched. This corresponds to the strict convexity of the integrand (2) in a neighborhood of the identity. For demonstrating this, we use the simple 2D shapes of Figure 4 and compare the matching of a circle with an ellipse, once solely using the volumetric elastic energy from (9) and once using our model energy (5) with membrane energy but without bending energy ($\alpha_{mem} = 1$, $\alpha_{\mathrm{bend}} = 0$). The resulting tangential distortion measures are presented in Table 1. In Figure 4, we show the resulting matching for our model.

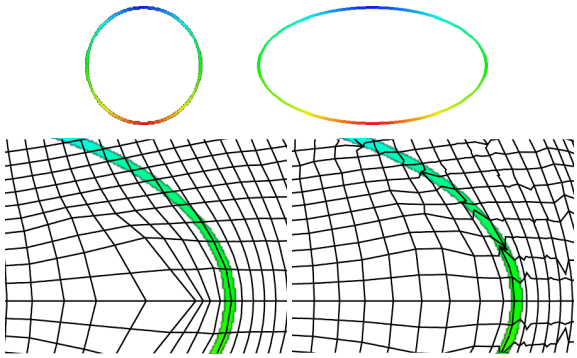

Figure 4: *Matching problem to explore the redistribution of tangential strain induced by the membrane term. Upper row: Reference and template shapes (colors are the same at the undeformed position on the circle and the deformed position on the ellipse). Lower row: detail of the deformed grid, drawn over the template shape. On the left side, only the volumetric elastic energy has been used, whereas in the right side we have used our model without bending energy (Table 1). Observe the localized deformations in the tangential direction to ensure the equidistribution of tangential strain.*

Level (h^{-1})	$\mathcal{E}_{\text{vol}}$ only	$\mathcal{E}_{\text{sh}}$ with $\alpha_{\text{bend}} = 0$
5 (33)	0.8541	0.1758
6 (65)	0.7949	0.0875
7 (129)	0.8053	0.0440
8 (257)	0.7953	0.0234
9 (513)	0.7978	0.0143

Table 1: *Standard deviation of the tangential strain on the narrow band* $2^{-\frac{1}{2}}\|\mathcal{D}_1\phi^T\mathcal{D}_1\phi\chi_{\{|d_1|<h\}}\|_F$ *around the reference curve. The ratio between length of the ellipse and length of the circle is* ≈ 2.38. *When using only a volumetric elasticity term, the deformation is basically a stretching in horizontal direction with large variation of the tangential strain, whereas in our model the strain is asymptotically equidistributed with decreasing grid size.*

Crumpling when minimizing only the membrane energy. One of the main limitations of using nonlinear membrane terms of the type (1), that strongly penalize compression, is that when trying to force a deformation from one shape to a thin neighborhood of a much smaller one, crumpling becomes unavoidable. Rather than a problem with our particular model, this is an issue with any realistic physical formulation, as crumpling occurs when crushing a sheet of paper, for example. If a very strong compression is required to match the reference to the template, oscillations are created to accommodate the excess of length. In this case, the continuous energy has no minimizer. We present a numerical example in

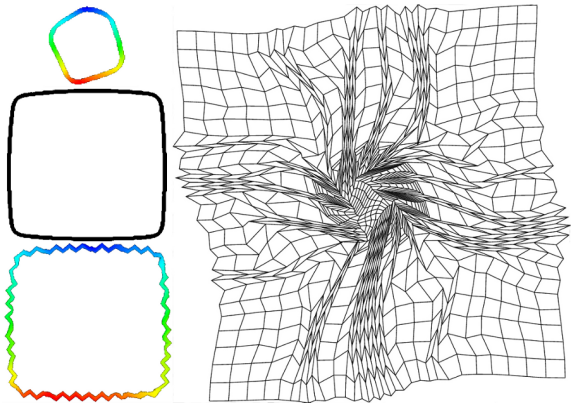

Figure 5: *Numerical crumpling on a coarse grid (*33^2 *points). Left column, top to bottom: Template curve, reference curve, and pullback of the template curve under the deformation* ϕ. *Right: Grid deformed through* ϕ.

which crumpling appeared in Figure 5. In fact, in this case the penalty parameter ε is not small enough to prevent the crumpling from being visible. This phenomenon was also observed in [HRWW12], for very small bending resistance.

Shape sensitive matching using the bending energy. We present two examples to underline the importance of the curvature matching term in Figure 6. In the first example, we aim at matching two rotated versions of a rounded l^1 ball. Without incorporating the curvature matching term E_{bend} ($\alpha_{\text{bend}} = 0$), the corners are squashed in one position and grown in another via the deformation. When E_{bend} is activated, the method finds the right rotation, because the rounded edges have to be mapped onto each other to reduce the norm of the relative shape operator.

The second example shows the matching of two different sections of an unduloid. Unduloids are surfaces of constant mean curvature first derived by Delaunay [Del41]. We attempt this both with the proposed bending energy (3), and a simpler mean curvature comparison term of the form

$$\mathcal{E}_{\text{bend}}^{\text{simple}} = \int_\Omega \eta_\sigma(\mathbf{d}_1)|H_2 \circ \phi - H_1|^2 \, dx, \tag{10}$$

as in [LDRS05], where H_i is the mean curvature of the surface $\mathcal{M}_i^{\mathbf{d}_i}$. Clearly, taking into account just a comparison of mean curvatures with the above energy is not appropriate, whereas the proposed shape operator alignment (3) matches the surfaces correctly.

Applications for shape matching. As a further proof of concept, we investigate a couple of matching problems in the context of more complicated shapes in Figures 7, 8 and 9. In particular, we investigate the performance of the cascadic descent and depict matching results on different grid levels in Figures 7 and 9. In all these applications, we have used the full variational model presented above (in Figure 8 and 9 in comparison with the results for a pure volume matching energy).

7. Conclusions and future work

We have presented a variational method for the matching of implicit surfaces represented as level sets. The proposed energies penalize both stretching / compression and bending of the surfaces via physically realistic elastic energies. The level set approach allows a formulation with only first order derivatives, and computation on regular grids. We have demonstrated qualitative properties for a set of simple test cases and show the applicability of the chosen approach for more complex surfaces. In particular, we have shown correct matches in cases where simpler elastic approaches fail.

A future research direction is to define shape spaces of such implicit shells (cf. [HRWW12] for the case of triangulated shell surfaces). Furthermore, a rigorous mathematical analysis of the model has to be developed, with criteria for the existence of minimizing deformations. Moreover, adaptive meshes would allow to treat much more detailed surfaces as they appear for instance in biological and medical applications.

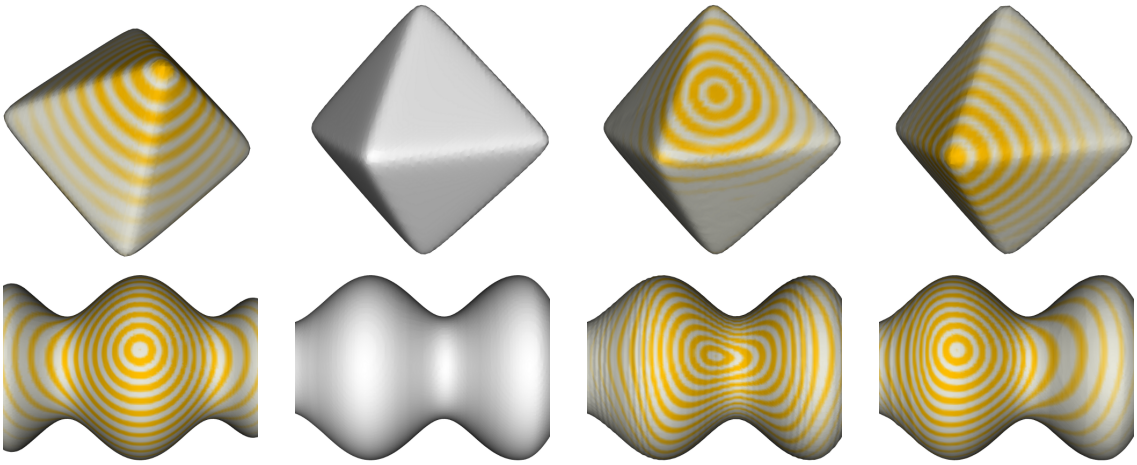

Figure 6: *Upper row: Effect of the bending energy $\mathcal{E}_{bend}$. From left to right: Textured template shape, reference shape, deformed template (with a push forward of the template texture) based on a matching with $\alpha_{bend} = 0$, deformed template with $\alpha_{bend} = 1$. Lower row: Matching of constant mean curvature surfaces. From left to right: Textured template shape, reference shape, deformed template using the energy $\mathcal{E}_{bend}^{simple}$, deformed template using a direct comparison of the shape operators via $\mathcal{E}_{bend}$.*

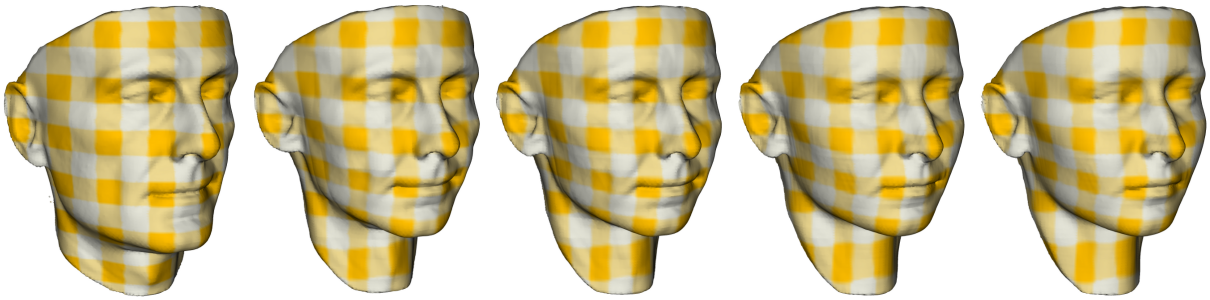

Figure 7: *From left to right: Textured template shape, and resulting deformed template after different stages of the cascadic minimization scheme (on 17^3, 33^3, 65^3, 129^3 grids, respectively).*

Acknowledgements

This research was supported by the Austrian Science Fund (FWF) through the National Research Network 'Geometry+Simulation' (NFN S117). The dinosaur and dolphin shapes were taken from the McGill 3D Shape Benchmark [SZM*08]. The scanned faces are part of the 3D Basel Face Model data [PKA*09].

References

[BMR13] BURGER M., MODERSITZKI J., RUTHOTTO L.: A hyperelastic regularization energy for image registration. *SIAM J. Sci. Comput. 35*, 1 (2013), B132–B148. 1

[BNP10] BONITO A., NOCHETTO R. H., PAULETTI M. S.: Parametric FEM for geometric biomembranes. *J. Comput. Phys. 229* (2010), 3171–3188. 2

[BPW12] BREDIES K., POCK T., WIRTH B.: Convex relaxation of a class of vertex penalizing functionals. *J. Math. Imaging Vis.* (2012). 2

[CFK04] CHARPIAT G., FAUGERAS O., KERIVEN R.: Approximations of shape metrics and application to shape warping and empirical shape statistics. *Found. Comp. Math. 5* (2004), 1–58. 2

[Cia88] CIARLET P. G.: *Mathematical elasticity, volume I: Three-dimensional elasticity*. North-Holland, Amsterdam, 1988. 2

[Cia00] CIARLET P. G.: *Mathematical elasticity, volume III: Theory of shells*. North-Holland, Amsterdam, 2000. 2, 3

[CPSS10] CHAO I., PINKALL U., SANAN P., SCHRÖDER P.: A simple geometric model for elastic deformations. *ACM Trans. Graph. 29* (July 2010), 38:1–38:6. 1

[Del41] DELAUNAY C.: Sur la surface de révolution dont la courbure moyenne est constante. *J. Math. Pures Appl.* (1841), 309–314. 6

[DZ94] DELFOUR M. C., ZOLÉSIO J.-P.: Shape analysis via oriented distance functions. *J. Funct. Anal. 123* (1994), 129–201. 2

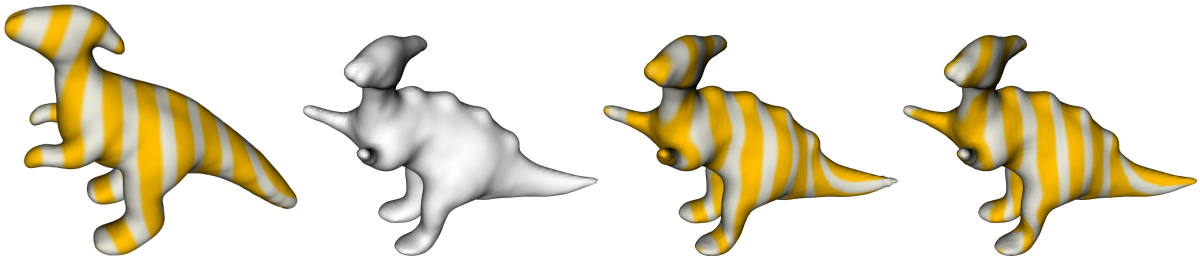

Figure 8: *From left to right: textured template surface, reference input surface, matching results for the full model on a* 129^3 *grid (with a push forward of the texture), analogous result with only volume elastic regularization and no shell registration energy. Without the membrane and bending terms, several parts are incorrectly matched (front of the head, both pairs of legs).*

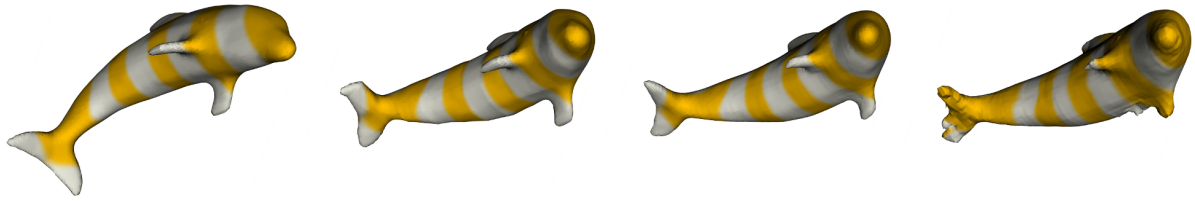

Figure 9: *From left to right: Textured template shape, resulting deformed template after minimization on a grid with* 17^3 *nodes and on a grid with* 129^3 *nodes, respectively, when using the full proposed model. Right most image: matching results based on a purely elastic volume matching. In particular, we observe artifacts due to a lack of surface deformation energies.*

[DZ95] DELFOUR M. C., ZOLÉSIO J.-P.: A boundary differential equation for thin shells. *J. Differential Equations 119*, 2 (1995), 426–449. 2

[EG92] EVANS L. C., GARIEPY R. F.: *Measure theory and fine properties of functions*. CRC Press, Boca Raton, 1992. 4

[FJM06] FRIESECKE G., JAMES R. D., MÜLLER S.: A hierarchy of plate models derived from nonlinear elasticity by gamma-convergence. *Arch. Ration. Mech. Anal. 180*, 2 (2006), 183–236. 3

[FJMM03] FRIESECKE G., JAMES R. D., MORA M. G., MÜLLER S.: Derivation of nonlinear bending theory for shells from three-dimensional nonlinear elasticity by Gamma-convergence. *C.R.A.S. Ser. I: Math 336*, 8 (2003), 697 – 702. 3

[FJSY09] FUCHS M., JÜTTLER B., SCHERZER O., YANG H.: Shape metrics based on elastic deformations. *J. Math. Imaging Vis. 35*, 1 (2009), 86–102. 2

[HRWW12] HEEREN B., RUMPF M., WARDETZKY M., WIRTH B.: Time-discrete geodesics in the space of shells. *Computer Graphics Forum (Proc. SGP) 31*, 5 (2012), 1755–1764. 6

[LDR96] LE DRET H., RAOULT A.: The membrane shell model in nonlinear elasticity: A variational asymptotic derivation. *J. Nonlinear Sci. 6* (1996), 59–84. 3

[LDRS05] LITKE N., DROSKE M., RUMPF M., SCHRÖDER P.: An image processing approach to surface matching. In *Symposium on Geometry Processing* (2005), Desbrun M., Pottmann H., (Eds.), pp. 207–216. 2, 6

[LL08] LEE T.-Y., LAI S.-H.: 3D non-rigid registration for MPU implicit surfaces. In *CVPR Workshop on Non-Rigid Shape Analysis and Deformable Image Alignment* (2008). 2

[Mod04] MODERSITZKI J.: *Numerical Methods for Image Registration*. OUP Oxford, 2004. 2

[MR12] MUKHERJEE D. P., RAY N.: Contour interpolation using level-set analysis. *Int. J. Img. Graph. 12*, 1 (2012), 1250004. 2

[NW06] NOCEDAL J., WRIGHT S.: *Numerical Optimization*, second ed. Springer, 2006. 5

[PKA*09] PAYSAN P., KNOTHE R., AMBERG B., ROMDHANI S., VETTER T.: A 3D face model for pose and illumination invariant face recognition. In *Proc. Advanced Video and Signal based Surveillance* (2009). 7

[PR02] PREUSSER T., RUMPF M.: A level set method for anisotropic geometric diffusion in 3D image processing. *SIAM J. Appl. Math. 62*, 5 (2002), 1772–1793. 4

[RW09] RUMPF M., WIRTH B.: A nonlinear elastic shape averaging approach. *SIAM J. Imaging Sci. 2*, 3 (2009), 800–833. 1

[Set99] SETHIAN J. A.: *Level set methods and fast marching methods*, second ed. Cambridge University Press, 1999. 3, 4

[SSJD09] SRIVASTAVA A., SAMIR C., JOSHI S. H., DAOUDI M.: Elastic shape models for face analysis using curvilinear coordinates. *J. Math. Imaging. Vis. 33* (2009), 253–265. 2

[SZM*08] SIDDIQI K., ZHANG J., MACRINI D., SHOKOUFANDEH A., BOUIX S., DICKINSON S.: Retrieving articulated 3-D models using medial surfaces. *Machine Vision and Applications 19*, 4 (2008), 261–275. 7

[WBRS11] WIRTH B., BAR L., RUMPF M., SAPIRO G.: A continuum mechanical approach to geodesics in shape space. *Int. J. Comput. Vis. 93*, 3 (2011), 293–318. 1

[WSSC11] WINDHEUSER T., SCHLICKEWEI U., SCHMIDT F. R., CREMERS D.: Geometrically consistent elastic matching of 3D shapes: A linear programming solution. In *International Conference on Computer Vision* (2011), pp. 2134–2141. 2